



Synthesis of six-coordinate mono-, bis-, and tris(tetrazolato) complexes via [3+2] cycloadditions of nitriles to silicon-bound azido ligands

Journal:	<i>Dalton Transactions</i>
Manuscript ID	DT-ART-07-2016-002867.R1
Article Type:	Paper
Date Submitted by the Author:	18-Sep-2016
Complete List of Authors:	Portius, Peter; The University of Sheffield, Chemistry Davis, Martin; The University of Sheffield, Chemistry

Synthesis of six-coordinate mono-, bis-, and tris(tetrazolato) complexes *via* [3+2] cycloadditions of nitriles to silicon-bound azido ligands

Peter Portius,^{*a} Martin Davis^a

Received (in XXX, XXX) Xth XXXXXXXXX 200X, Accepted Xth XXXXXXXXX 200X

First published on the web Xth XXXXXXXXX 200X

DOI: 10.1039/b000000x

Abstract. A convenient synthetic route to poly(tetrazolato) silicon complexes is described based on the four reactive centres of the N-rich, highly endothermic tetraazides of the type Si(N₃)₄(L₂). Hypercoordinate azido(tetrazolato) silicon complexes Si(N₃)₂(N₄C-R)(L₂), R = CH₃, C₆H₅, 4-C₆H₄CH₃ (**4a**, **5**, **6**, **7**) and Si(N₃)₂(N₄C-L)₂ (**9**, L = 2-C₅H₄N, L₂ = 2,2'-bipyridine, 1,10-phenanthroline, with SiN₆ skeletons were synthesised *via* multiple [3+2] dipolar cycloaddition reactions starting from Si(N₃)₄(L₂) and a nitrile. The isolated new complexes were characterised by standard analytical methods, single crystal X-ray diffraction and Differential scanning calorimetry (**4a**, **b**). Tetrazolato ligand linkage isomerism was observed for complex **4a**. The crystallographically characterised methyl tetrazolato complexes and plausible configurational and linkage isomers were evaluated by DFT calculations on the B3LYP/6-311G(d,p) level.

Introduction

Tetrazoles play an important role as versatile ligands in coordination chemistry of transition metals and lanthanides (see refs. 1-3 and the literature cited therein) where their complexes are used as spin crossover materials,⁴ antitumor agents,⁵ gas generants⁶ and energetic material.⁷ Large positive heats of formation, large volumes of dinitrogen generated upon thermal decomposition and the potential for comparably high thermal stability make nitrogen-rich (N-rich) tetrazolato metal complexes attractive targets for application as energetic materials and N₂ generants.⁷⁻¹⁶ For instance, metal-free N-rich compounds are a desirable replacement for lead azide as they avoid the deleterious environmental impact of heavy metals,^{7,9,14,17} and thus are promising precursors for new binary element-nitrogen materials.¹⁸ N-rich tetrazole complexes of silicon are particularly interesting as silicon is cheap, abundant, non-toxic and amenable to hyper coordination. However, the lesser metallic character of silicon requires the development of new synthetic strategies to introduce N-rich ligands.

In general, coordination compounds of *p*-block elements bearing tetrazolato ligands can be synthesised by a number of methods. These include Lewis base assisted HX elimination (*i*),^{19,20,21} oxidative addition of tetrazole (*ii*),²² Brønsted acid-base reaction (*iii*),^{8,23} thermally activated [3+2] cycloaddition of mono(azido)silanes and aryl or alkyl nitriles (*iv*),²⁴⁻²⁶ and silylation (*v*),²⁷ resulting in 5-substituted tetrazole derivatives with the exception of method (*v*). Compounds in which *one* tetrazolyl group is bound directly to silicon are represented by several dozens of examples, including silanes²⁸ SiMe₃(κN(2)-mtz),^{28,29} SiMe₃(κN(2)-5-R-tz),³⁰ SiMe₃(κN(2)-ptz),^{30,31,44} SiMe₃(tz-NH-SiMe₃),³¹ SiMe₃(κN(1)-tz-CX₃),³² SiMe₃(κN(1)-ptz),³³ SiMe₃(κN(1)-tz-OSiMe₃),^{34,35} SiMe₃(κN(1)-tz-NH-SiMe₃),³¹ SiMe₃(κN(1)-htz),^{27,31} SiMe₂H(κN(1)-htz)²¹ and SiMe₂{C(SiMe₂Ph)₃}(κN(2)-mtz)²⁸ and the hexacoordinate Si(salen)(Ph)(κN(2)-ptz)²² (tz = tetrazolyl, htz = 5-H-CN₄, mtz = 5-Me-CN₄, ptz = 5-Ph-CN₄, salen = bis(salicyliden)ethylenediamin, R = Et, Ph, CH₂Ph, X = F, Cl). However, *poly*(tetrazolyl) compounds and higher-coordinated complexes bearing tetrazolato ligands and main

group elements as coordination centres are extremely rare (for an overview of higher-coordinated molecular silicon compounds see refs. 36-41 and the literature cited therein). To the best of our knowledge $\text{SiMe}_2(\kappa\text{N}(1)\text{-htz})_2$,²¹ $[\text{BH}_2(\kappa\text{N}(1)\text{-5-R-tz})_2]^-$,^{8,23} $[\text{E}(\text{por})(\text{ptz})_2]$ E = Ge, Sn,⁴² and $[\text{Si}(\text{salen})(\text{Ph})(\kappa\text{N}(2)\text{-ptz})]^{22}$ are the only four examples reported. The cited literature provides NMR,⁴³⁻⁴⁵ X-ray crystal and electron gas phase diffraction⁴⁰ and reactivity data.^{29,41-43} The experimental investigation⁵⁰⁻⁵² of N-rich tetrazolato complexes poses primarily two challenges: the potential for high energy density, percussion sensitivity and thermal lability and the fact that most *p*-block element-tetrazole compounds are prone to hydrolysis.⁵³⁻⁵⁶

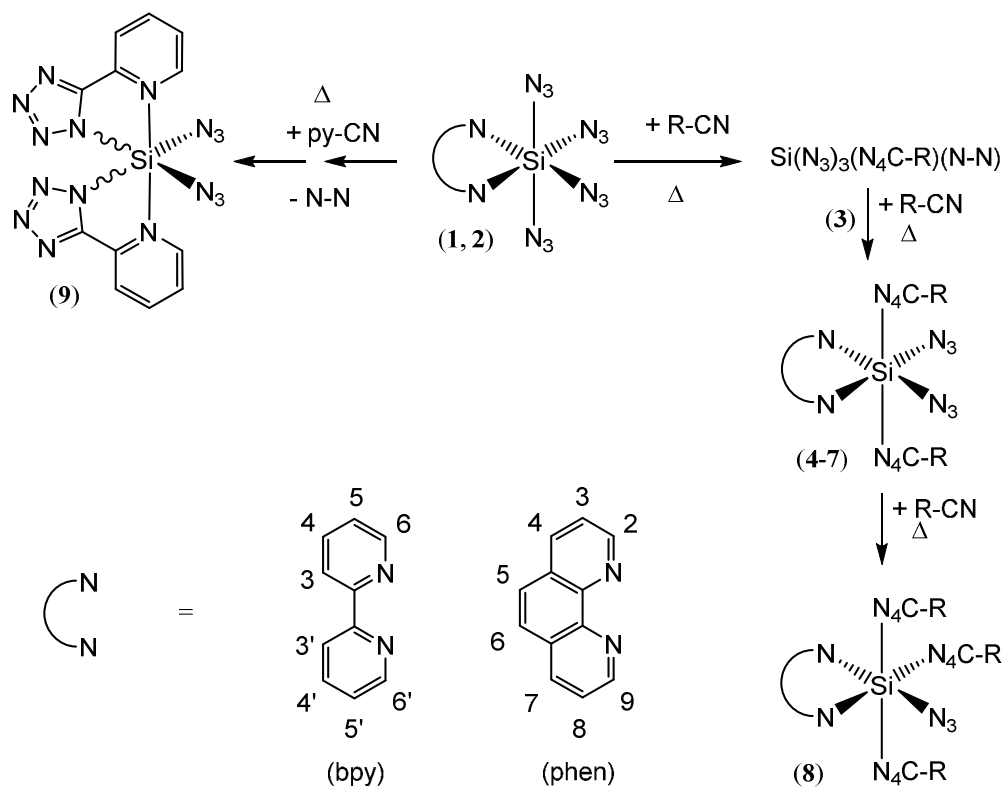
In this paper we describe a convenient synthetic route to poly(tetrazolato) complexes based on the intriguing four reactive centres of the previously described N-rich, highly endothermic tetraazides of the type $\text{Si}(\text{N}_3)_4(\text{L}_2)$,⁵³ $\text{L}_2 = 2,2'$ -bipyridine (bpy), 1,10-phenanthroline (phen);^{51,52,57,58} see ref. 24 for recent reviews of azido complexes chemistry. The new method allows for the synthesis and isolation of unusual hyper-coordinate poly(tetrazolato) poly(azido) silicon complexes, where two types of N-rich ligands are combined on one centre and where the number of N_3 ligands engaging in cycloaddition with nitrile forming tetrazolato ligand can be varied from one to three by careful adjustment of reaction conditions. The structural, spectroscopic and thermal properties of the new complexes are described including a discussion of their propensity to linkage isomerism.

Results

In sealed vessels, the colourless solutions of tetraazido complexes $\text{Si}(\text{N}_3)_4(\text{bpy})$ (**1**) and $\text{Si}(\text{N}_3)_4(\text{phen})$ (**2**) in the nitriles R-CN (R = Me, Ph, 4-tol, 2-py) show no signs of decay over several weeks at r.t.¹ However, at temperatures ranging from 90 °C to 150 °C reactions can be induced² the course of which was monitored by IR spectroscopy. Over the course of several hours changes in the spectral range of the asymmetric azido group stretching vibration, $\nu_{\text{as}}(\text{N}_3)$, occur. The bands arising from the starting complexes **1** or **2** are replaced gradually by those of intermediates and products (Scheme 1, Table 1, Fig. 1).

¹ MeCN solution can be kept for weeks without noticeable degradation.

² With the exception of py-CN which is a solid at r.t.



Scheme 1. Syntheses of the poly(tetrazolato)poly(azido)silicon complexes $[\text{Si}(\text{N}_3)_3(\text{ptz})(\text{phen})]$ (3), $[\text{Si}(\text{N}_3)_2(\text{mtz})_2(\text{bpy})]$ (4), $OC-6-13-[\text{Si}(\text{N}_3)_2(\kappa\text{N}(2)\text{-ptz})_2(\text{bpy})]$ (5), $OC-6-13-[\text{Si}(\text{N}_3)_2(\kappa\text{N}(2)\text{-ttz})_2(\text{bpy})]$ (6), $OC-6-13-[\text{Si}(\text{N}_3)_2(\kappa\text{N}(2)\text{-ptz})_2(\text{phen})]$ (7), $OC-6-31-[\text{Si}(\text{N}_3)(\text{mtz})_3(\text{bpy})]$ (8) and $OC-6-22-[\text{Si}(\text{N}_3)_4(\text{bpy})]$ (9) from $OC-6-22-[\text{Si}(\text{N}_3)_4(\text{phen})]$ (1) and $OC-6-22-[\text{Si}(\text{N}_3)_4(\text{phen})]$ (2) with R-CN; R = 5-Me (mtz), 5-Ph (ptz); 5-(tol-4'-yl) (ttz), 5-(pyrid-2'-yl) (pytz).

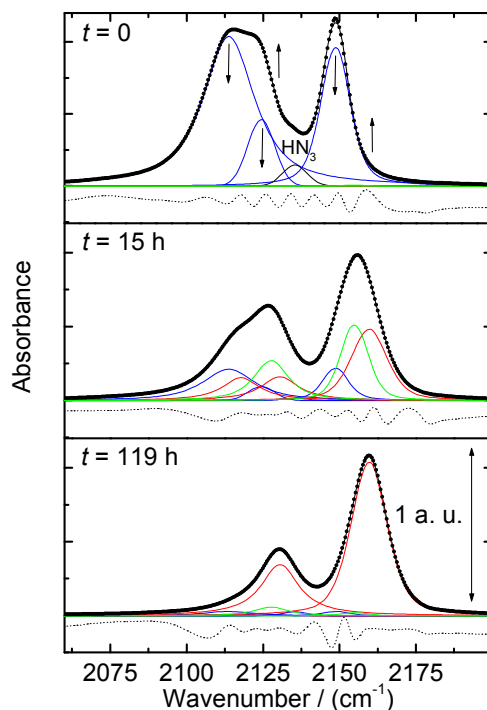


Fig. 1. *In-situ* FTIR spectra (dots) of the $\text{Si}(\text{N}_3)_4(\text{phen})$ (2) - PhCN reaction solution after initiation (top), 15 h (middle) and 119 h heating time (bottom). Blue, green and red curves indicate absorptions from complexes 1, 3, 8,

and **7**, respectively as components of a fit to the experimental spectrum (black line) using *pseudo*-Voigt profiles attributed to bands of each species, which was optimised by the least squares method. The fit residuals (x10) are shown in the off-set.

Table 1. Wavenumbers of the asymmetric azido ligand stretching vibrations, $\nu_{\text{as}}(\text{N}_3)$, in the complexes **1** to **9**

Complex	$\bar{\nu}$ / (cm^{-1}) (in paraffin)	$\bar{\nu}$ / (cm^{-1}) (in MeCN)	Ref.
1	2151m, 2142s, 2114 vs, 2103vs	2151s, 2126s, sh, 2116vs	^c
2	2147vs, 2121vs, 2113s, 2102w	2150vs, 2126s, sh, 2118vs	^c
3	2152vs, 2117vs	2155vs, 2128w, 2118s ^a	^d
4a	2149vs, 2122s	2163vs, 2132w ^b	^d
4b	2157vs, 2122m	2163vs, 2132w ^b	^d
5	2166vs, 2126s	2162vs, 2132w	^d
6	2156vs, 2127s	2162vs, 2132w	^d
7	2164vs, 2158vs, 2129vs	2162vs, 2132w	^d
8	2158vs	2159vs	^d
9	2164vs, 2122s	2142s	^d

^a in PhCN solution, ^b in MeCN solution, the in-phase and out-of-phase $\nu_{\text{as}}(\text{N}_3)$ stretches, respectively, of the **4a,b** equilibrium mixture are not unresolved, ^c see ref. 52, ^d this paper.

The energies of the vibrational bands attributed to the transients are in the range typical for coordinated N_3 groups, indicating the involvement of long-lived azido complexes. Figure 1 shows *in situ* IR spectra recorded as a function of time as an example of the spectral evolution typical for these reactions. Spectral line-shape analysis revealed that in the spectrum recorded 15 h after reaction initiation, five new $\nu_{\text{as}}(\text{N}_3)$ bands centred at 2118, 2128, 2130, 2155 and 2160 cm^{-1} are present. Prolonged reaction time causes the bands at 2130 and 2160 cm^{-1} to grow whereas those at 2118, 2128 and 2155 cm^{-1} decay. The latter bands are therefore assigned to an intermediate complex (**3**), whereas those that remain belong to complex **7** (*vide infra*, Fig. S8). Analogous observations have been made upon monitoring the reaction of complex **1** with PhCN by ^1H NMR spectroscopy. The *in situ* ^1H NMR spectra exhibit three resonances for the bpy protons H(6) and H(6') at 9.40 ppm (**1**), 9.69 ppm (**3**) and 9.93 ppm (**5**) the relative signal intensities of which depend on the reaction progress, with the latter one being the major component in the final stages of the reaction (see Figs 2-4). Similarly, spectra recorded of the reaction mixture of complex **2** in PhCN show three resonances of the phen protons H(2) and H(9) at 9.60 ppm (**2**), 9.93 ppm (intermediate) and 10.17 ppm (**7**) with the latter being the major component in the last stages of the reaction. The reactions with MeCN lead to more complex spectra. The reaction of **1** produces two resonances of unequal intensity characteristic of the bpy protons H(6) and H(6') at 9.84 ppm and 9.59 ppm, respectively (complex **2** as starting material resulted in the phen H(2) and H(9) resonances at 9.65 ppm and 10.07 ppm). At least two intermediates could be identified at 9.64 ppm and 9.32 ppm (reactant **1**) and 9.85 ppm and 9.57 ppm (reactant **2**). Upon prolonged heating, the intermediate signals vanished while the ratio of the two product signals remained unchanged. An interpretation of these findings was obtained by a combination of mass spectrometry, X-ray crystallography and DFT calculations (*vide infra*).

In all cases the reactions could be driven nearly selectively to completion (see Scheme 1) leading to the compounds **4**, **5**, **6**, **7** and **9**, which were isolated by crystallisation from MeCN as colourless

crystals in yields ranging from 35% to 87%. While the crystalline compounds are only slightly air sensitive, solutions hydrolyse readily upon exposure to air. The new compounds are less soluble in MeCN, THF and CH₂Cl₂ than the starting complexes and exhibit similar thermal stability, decomposing at temperatures ranging from 201°C (**7**) to 231°C (**4**).

¹H NMR spectra of the non-volatile product of the reaction of complex **1** with MeCN after several hours show the presence of two mirror-symmetric bpy bearing methyl-tetrazolato (mtz) complexes as evidenced by the two doublet resonances arising from bpy 6 and 6' protons. The ¹H CH₃ resonances of the mzt ligands have chemical shifts at 2.20, 2.21 and 2.80 ppm. Crystallisation under carefully chosen conditions afforded crops of crystals of two different complexes **4a** and **4b**, the latter being obtained from the mother liquid of the former. The reactant nitriles can also bear Lewis bases, such as in 2-pyridyl nitrile, 2-py-CN. At 120°C complex **2** dissolves in a melt of 2-py-CN and reacts within 12 hours to form complex **9**. The combination of IR and NMR data strongly suggests that the tris(azido) complexes *OC-6-23*-[Si(N₃)₃(Rtz)(L₂)], R = Ph, Tol; L₂ = bpy, phen, dominate the long-lived intermediates *en route* to the product complexes. Further evidence for the formation of intermediates was obtained by arresting the reaction at an early stage (cooling the reaction mixture to r.t.) by which a solid was obtained consisting mainly of complex **3**. Mass spectrometric as well as ¹H NMR and IR data of this material indicate that the [3+2] cycloaddition leads to the structure indicated in Scheme 1.

Crystals of the complexes **4a,b**, **5**, **6**, **7** and **9** suitable for single crystal X-ray diffraction studies were obtained by cooling or slowly evaporating concentrated acetonitrile solutions (see Table 2). The crystalline compounds consist of hexacoordinate silicon complexes with a SiN₆ coordination skeleton (see refs. 59-63 for related [SiN₆] complexes). With the exception of **9**, the central silicon atom is coordinated by two tetrazolato ligands, two azido ligands and the bidentate bpy or phen ligand with *OC-6-13* configuration in which both tetrazolato ligands coordinate *trans* throughout, while the azido ligands are coordinating *cis* to one another but *trans* with respect to the bidentate ligands. The complexes **4a** (Fig. 2, R = Me), **5** (R = Ph, not shown), **6** (Fig. 3, R = Tol) and **7** (Fig. 3, R = Ph) feature the tetrazolato ligands coordinating *via* the N(2) nitrogen atom exclusively.

Table 2. Summary of crystal data and refinement results for the complexes **4a,b**, **5**, **6**, **7-CH₃CN** and **9**.

complex	4a	4b-CH₃CN	5	6-CH₃CN	7-CH₃CN	9
sumf.	C ₁₄ H ₁₄ N ₁₆ Si	C ₁₆ H ₁₇ N ₁₇ Si	C ₂₄ H ₁₈ N ₁₆ Si	C ₂₈ H ₂₅ N ₁₇ Si	C ₂₈ H ₂₁ N ₁₇ Si	C ₁₂ H ₈ N ₁₆ Si
<i>M</i> /(g mol ⁻¹)	434.50	475.56	558.63	627.74	623.71	404.43
crystal symmetry	monoclinic	monoclinic	monoclinic	monoclinic	triclinic	ortho-rhombic
space group	<i>C</i> 2/c	<i>P</i> 2(1)/c	<i>C</i> 2/c	<i>P</i> 2(1)/c	<i>P</i> 1	<i>P</i> bcn
<i>a</i> / Å	11.7941(6)	10.8760(3)	22.7377(5)	10.8508(6)	11.1045(3)	12.030(4)
<i>b</i> / Å	13.5508(6)	14.5601(4)	10.33383(2)	24.9343(6)	11.9991(4)	9.833(3)
<i>c</i> / Å	12.6135(6)	14.9281(4)	10.6088(2)	11.6091(6)	12.7949(4)	13.979(4)
<i>α</i> / °	90	90	90	90	96.060(1)	90
<i>β</i> / °	104.555(2)	110.732(2)	99.218(1)	110.092(2)	108.545(1)	90
<i>γ</i> / °	90	90	90	90	111.168(1)	90
<i>V</i> / Å ³	1951.19(16)	2210.87(10)	2461.60(9)	2949.8(3)	1459.66(8)	1653.6(9)

Z	4	4	4	4	2	4
$D_C / (\text{Mg m}^{-3})$	1.479	1.429	1.507	1.414	1.419	1.624
T / K	130(2)	96(2)	87(2)	100(2)	100(2)	110(2)
$\mu(\text{Mo-K}\alpha) / (\text{mm}^{-1})$	0.163	0.152	0.148	0.133	0.134	0.185
R_1	0.0316	0.0473	0.0436	0.0494	0.0359	0.0442
wR_2	0.0837	0.1070	0.1307	0.1208	0.0977	0.0999

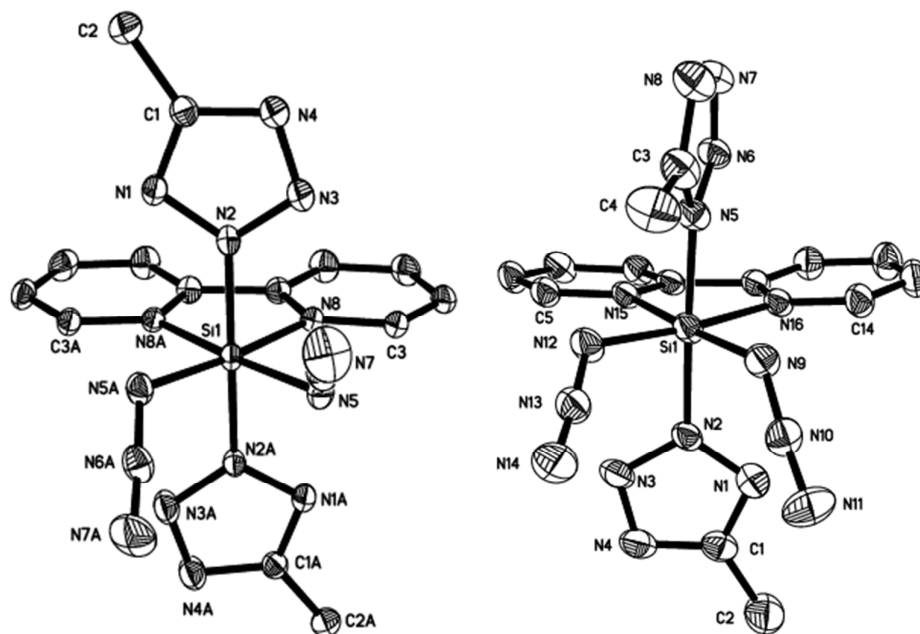


Fig. 2. Thermal ellipsoid plots of *OC-6-13*-[Si(N₃)₂(κN(2)-mtz)₂(bpy)] (**4a**, left) and *OC-6-24*-[Si(N₃)₂(κN(1)-mtz)(κN(2)-mtz)(bpy)] co-crystallised with MeCN (**4b**, right) drawn at the 50% probability level. H atoms and MeCN have been omitted for clarity. Selected bond lengths [Å] and angles [°] **4a**: Si1-N5 1.804(1), Si1-N2 1.895(1), Si-N8 1.940(1), N5-N6 1.219(2), N6-N7, 1.137(2), Si-N5-N6 120.24(9), N5-Si1-N5A 96.42(5); **4b**: Si1-N9 1.816(2), Si1-N12 1.802(3), Si1-N2 1.901(3); Si1-N5 1.868(3); N12-N13 1.211(3), N13-N14 1.143(3), N9-N10 1.219(3), N10-N11 1.138(3), Si1-N15 1.944(2), Si1-N16 1.936(3), Si1-N12-N13 123.9(2), Si1-N9-N10 127.3(2), N9-Si1-N12 96.8(1).

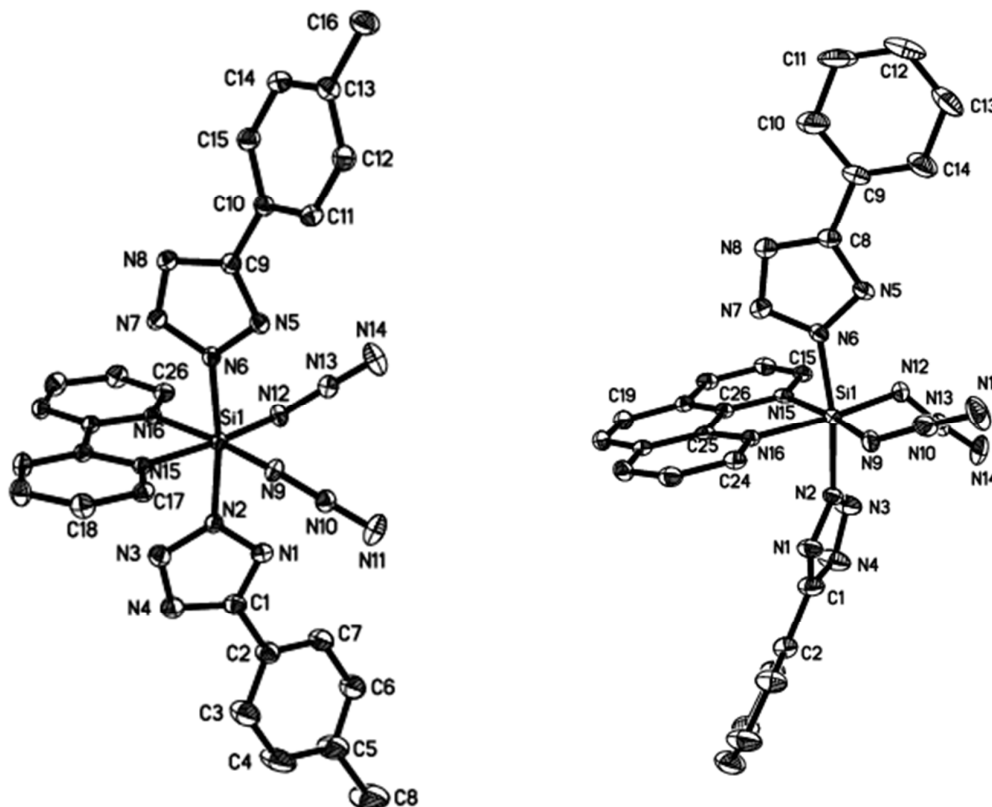


Fig. 3. Thermal ellipsoid plots of *OC-6-13*-[Si(N₃)₂(κN(2)-ttz)₂(bpy)] co-crystallised with MeCN (**6**, left) and *OC-6-13*-[Si(N₃)₂(κN(2)-ptz)₂(phen)] in the crystal of 7·CH₃CN (right) drawn at the 50% probability level. H atoms and MeCN have been omitted for clarity. Selected bond lengths [Å] and angles [°] **6**: Si1-N9 1.784(2), Si1-N12 1.796(3), Si1-N2 1.914(2), Si1-N6 1.897(2), Si1-N15 1.938(2), Si1-N16 1.943(2), N9-N10 1.225(3), N10-N11 1.136(4), N12-N13 1.217(4), N13-N14 1.145(4), Si1-N9-N10 126.1(2), Si1-N12-N13 125.9(2), N9-Si1-N12 97.6(1); **7**·CH₃CN: Si1-N9 1.811(3), Si1-N12 1.787(3), Si1-N2 1.896(2), Si1-N6 1.899(2), Si1-N15 1.964(3), Si1-N16 1.945(3), N9-N10 1.208(5), N10-N11 1.146(5), N12-N13 1.222(3), N13-N14 1.135(4), Si1-N12-N13 125.6(2), Si1-N9-N10 122.3(2), N9-Si1-N12 97.9(1).

In comparison with the available data on silicon tetrazolates, the coordinative bonds of the tetrazolato ligands (Si-N_T) are longer than in the tetracoordinate [Si{C(SiMe₂Ph)₃}Me₂(κN(2)-mtz)}] (*ca.* 1.984 Å)²⁸ but shorter than in the complex *trans*-[Si(κN(2)-ptz)(Ph)(κ⁴-salen)], 1.995(2) Å.²² This finding can be rationalised by an increased coordination number and the reduced electron donation capabilities of the *trans* ligand Ph vs. RCN₄. The N_T-Si-N_T angle included between the *trans* arranged tetrazolato ligands and the coordination centre ranges from 171° to 175° for all investigated complexes with the exception of complex **9**.

The structure of complex **9** (Fig. 4) is principally different and reveals the formation of 2-pyridyl tetrazolato ligands, which bind in a bidentate κ²N(1),N⁷ fashion displacing the 2,2'-bipyridyl ligand. The azido ligands coordinate *trans* to the tetrazolato groups (Fig. 4) resulting in an *OC-6-22* configuration. As opposed to the complexes bearing two monodentate tetrazolato ligands, the tetrazolato groups of the bidentate ligands coordinate in mutual *cis* arrangement with azido groups as *trans* ligands.

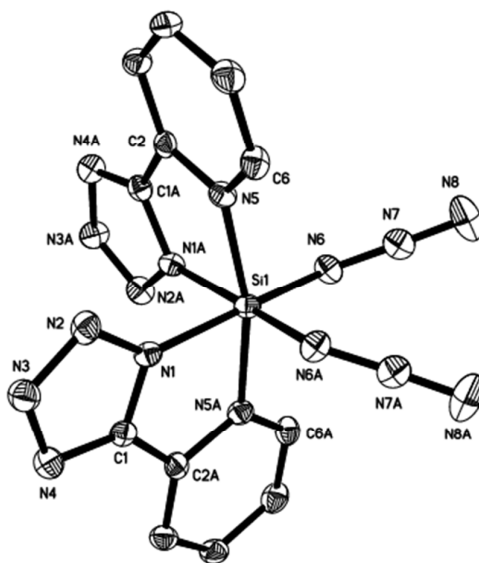


Fig. 4. Thermal ellipsoid plot of Δ -OC-6-22-[Si(N₃)₂(κ^2 N(1),N⁷-pytz)₂] (**9**) drawn at the 50% probability level. H atoms have been omitted for clarity. Selected bond lengths [Å] and angles [°]: Si1-N6 1.792(3), Si1-N5 1.940(2), Si1-N1 1.883(3), N6-N7 1.223(4), N7-N8 1.137(4), N6-Si1-N6A 99.0(1), Si1-N6-N7 136.5(2). Note the crystallographically imposed C₂ symmetry of the complex.

Complex **4b** features the unusual combination of two tetrazolato ligands coordinating *via* N(1) and N(2), respectively (Fig. 2). While the distance $d(\text{Si},\text{N}(2))$ remained nearly unchanged, the Si,N(1) bond lengths is shortened by approximately 3 pm (Tab. 2). A comparison of the tetrazolato complex structures with those of **1** and **2** (Table 3) shows that replacement of the axial azido by tetrazolato ligands induces a shortening of the coordinative Si-N bonds of both remaining azido as well as the bidentate ligands by 3.6 - 1.7 pm and 1.6 - 1.5 pm, respectively. This shortening is attributed mainly to the higher electron withdrawing effect of the tetrazolato ligand compared with the axial azido ligand *via* the coordinative Si-N σ bonds.⁶³ The azido ligand-internal N-N bond lengths differences, ΔNN , which can be used as an indicator for the iconicity of the coordinative Si-N₃ bond,^{51,52,58,64} range from 7.3 pm to 8.2 pm and thus reveal that the effect of the Si-N bond elongation on the structure of the azido ligands is insignificant. The silicon – tetrazole bond lengths, $d(\text{Si}-\text{N}_T)$, are affected only marginally by the tetrazole substituents R $\kappa\text{N}(1)(\text{N}_4\text{C-Me}) < \kappa\text{N}(1)(\text{N}_4\text{C-Ph/Tol})$ (**4a** vs. **5**, **6**) and the bidentate ligands phen < bpy (**5** vs. **7**). The linkage isomer **4b** (Fig. 2), however, features a 3 pm bond Si-N_T lengths difference whereby the Si- $\kappa\text{N}(1)(\text{N}_4\text{C-Me})$ bond is shorter and the Si- $\kappa\text{N}(2)(\text{N}_4\text{C-Me})$ bond longer than in the otherwise identical complex **4a**, hence the electronic effect dominates over the steric effect. The tetrazole ligand σ electron donating capability is clearly enhanced in the $\kappa\text{N}(1)$ coordination mode which causes shortening of the Si-N_T bond and, due to the *trans* influence, pushes the second tetrazolato ligand which coordinates in $\kappa\text{N}(2)$ away from the coordination centre compared to complex **4a**. As expected for a configuration with least steric interaction, the planes of all tetrazolato ligands are in a *gauche* configuration with respect to the adjacent four Si-N bonds.

Table 3. Selected bond lengths $d / \text{\AA}$ and angles $\alpha / ^\circ$ ^a

	1^f	2^f	4a	4b	5	6	7	9
Si-N _{α} ^b	1.826	1.834	1.804	1.809	1.794	1.790	1.800	1.792
N _{α} -N _{β}	1.214	1.211	1.219	1.215	1.214	1.221	1.215	1.223
N _{β} -N _{γ}	1.135	1.137	1.137	1.141	1.141	1.141	1.137	1.137
Δ NN ^c	0.079	0.074	0.082	0.075	0.073	0.081	0.078	0.086
Si-N _T ^d	-	-	1.895	1.868, 1.901	1.908	1.906	1.896	1.883
Si-N _{py} ^e	1.956	1.969	1.940	1.940	1.941	1.941	1.954	1.940
Si-N _{α} -N _{β}	123.6	121.0	120.2	125.6	125.1	126.0	124.2	136.5
N _{α} -Si-N _{α}	97.0	97.8	96.4	96.8	98.8	97.6	98.2	99.0
N _T -Si-N _T	172.0	173.7	172.8	175.2	172.6	172.5	171.1	87.1
N _{tet} -N _{tet} ^f	-	-	164	103.0	28	34	67	-

^a Estimated error margins (typically $\pm 0.001 \text{ \AA}$, 0.1°) omitted for clarity, see figure captions and ESI for full details; ^b N _{α} , N _{β} and N _{γ} denote the nitrogen atoms of the N _{α} bound azido ligand; ^c Δ NN = $d(\text{N}_{\alpha}\text{-N}_{\beta}) - d(\text{N}_{\beta}\text{-N}_{\gamma})$; ^d N_T denotes the coordinating nitrogen atom of the tetrazolato ligand; ^e N_{py} denotes the coordinating nitrogen atom of the pyridine-based ligands bpy, phen, N₄C-py; ^f torsion angle between the tetrazolato ring planes; ^f equatorial azido groups, see ref. 52.

The IR spectra (MeCN) of the bpy complexes **4a,b**, **5**, **6**, and **7** in MeCN exhibit two intense absorption bands due to the in-phase and out-of-phase asymmetric N₃ vibrations at 2162 - 2163 cm⁻¹ (intense) and at 2132 cm⁻¹ (weak), respectively, which are both at higher energies in comparison to those of the parent complex **1**. Their spectral position is insensitive to the type of the bidentate ligand, the tetrazole R group and the tetrazole coordination mode (see Table 1). This trend is adhered to by the analogous phen complexes **2** and **7** with the triazido complex **3** occupying an intermediate position. Finally, the substitution of azido by tetrazolato ligands is accompanied by an increase of the average $\nu_{\text{as}}(\text{N}_3)$ frequencies (2131 (**1**), 2134 (**3**), 2148 (**4a**), 2159 (**8**); see Table 4 for the calculated average frequencies 2258 (**1**), 2269 (**h**), 2282 (**a**), 2293 cm⁻¹ (**k**), respectively), which implies that the degree of covalence of the remaining Si-N₃ bonds increases with an increased number of coordinating tetrazolato ligands. This finding suggests that in the investigated complexes the tetrazolato ligand acts as a poorer σ donor than the azido ligand. There is no detectable influence of the bidentate ligand on the $\nu_{\text{as}}(\text{N}_3)$ frequencies (complex **5** vs. **7**). These findings indicate that the remaining Si-N₃ bonds strengthen with an increasing number of tetrazolato ligands, which is in line with the observed Si-N _{α} bond-lengths changes and confirms that the electron donating capability of the tetrazolato ligand is poorer in comparison to the azido ligand. The spectral positions of the bands arising from the in-phase and out-of-phase $\nu_{\text{as}}(\text{N}_3)$ stretching vibrations of complex **9** ($\bar{\nu} / (\text{cm}^{-1}) = 2164\text{vs}, 2122\text{s}$) are remarkably similar to those of complex **5** (2166vs, 2126s) despite the inverted arrangement of tetrazolato and pyridine ligands. A comparison of ²⁹Si NMR chemical shift data (complex **5**, $\delta = -190.5$ ppm) with previously reported complexes with skeletons such as SiN₆ and SiN₄X₂ (Si(N₃)₆²⁻,⁵¹ Si(X)₂L₂, X = F-Br, CN, NCO, NCS, S-R, Se-R, L = (iPrN)₂CPh⁴⁰), ranging from $\delta = -161$ to -217 ppm, shows that the shielding of the coordination centre is dominated by the nature of the coordination skeleton which causes a characteristic high field chemical shift around 190 ppm.

Linkage Isomerism

While the coordination geometry of complex **4a** resembles closely that of **5-7** (Fig. 3), **4b** is a linkage isomer of **4a** with both $\kappa N(1)$ and $\kappa N(2)$ -bound tetrazolato ligands present (Fig. 2). The in-phase $\nu_{as}(N_3)$ vibration shifts to higher energy, an effect clearly visible in the solid state IR spectra (Table 1). Crystals of each isomer can be dissolved in MeCN- d_3 and the NMR spectra of each isomer recorded; however, heating to 80°C causes linkage isomerisation and the rapid establishment (within less than an hour) of the same ratio of linkage isomers **4b** : **4a** in the reactions **4a** \rightarrow **4b** (*ca.* 0.88) and **4b** \rightarrow **4a** (*ca.* 0.84) in both samples made up of either pure **4a** or **4b**. This suggests a slight thermodynamic preference of **4a** over **4b** equal to about $\Delta G = -0.1$ to -0.8 kJ mol⁻¹. Due to the insufficient solubility of the tetrazolato complexes, neither ¹⁵N nor ²⁹Si NMR resonance could be observed in solution. Tetrazolato complexes can undergo $\kappa N(1)$ / $\kappa N(2)$ linkage isomerism, see for instance complexes of Co⁶⁵ and Si.³⁴ The energetics for a range of hexacoordinate azido(tetrazolato) tetrazolato complexes was investigated by *ab initio* methods (*vide infra*).

Tris(tetrazolato) complexes

While prolonged heating of the reaction solutions containing **5** and **9** lead to progressive yellow discolouration where no reaction products could be isolated, the reaction of **1** in MeCN leads *via* the isomers **4a** and **4b** within ten days to the precipitation of a white solid and the complete disappearance of $\nu_{as}(N_3)$ bands from the *in situ* IR spectra. A sparingly soluble white solid was obtained by filtration and washing of the precipitate as compound **8**, which features only a single ν_{as} absorption band at 2159 cm⁻¹. Crucially, the bpy H(6) and H(6)' as well as the mtz CH₃ protons are no longer isochronous, the latter one being indicative of axial $\kappa N(2)$ -mtz ligands (2.23 ppm) and of one other type of mtz ligand (2.40 ppm) in the ratio of 2 : 1. A 100% peak was observed in ES⁺ mass spectra at $m/z = 498$ Da, which arises from Na⁺ attachment to the molecular ion with the rational formula Si(N₃)(mtz)₃(bpy). The combined analytical data strongly suggest that the tris(tetrazolato) silicon complex with the structure OC-6-23-[Si(N₃)(mtz)₃(bpy)] (**8**) had formed, see Scheme 1. As yet, no evidence for the formation of any Si(L₂)(Rtz)₄ has been obtained. The available data does not permit conclusions regarding the mechanism of the azide-nitrile cycloaddition^{24,66} involving the investigated 6-coordinate complexes (which could, potentially, explain the reasons why the tetrakis(tetrazolato) silicon could not be prepared as yet).

Thermal Behaviour. The thermal behaviour of the diazido bis(tetrazolato) complexes **4a**, **8** and **9** was studied by differential scanning calorimetry (DSC), which showed no melting and a single, sharp exothermic decomposition with onset temperatures $T_{on}^{ex} = 242^\circ\text{C}$ ($T_p^{ex} = 253^\circ\text{C}$) (**4a**), 233°C (253°C) (**8**) and 223°C (273°C) (**9**), respectively (see Fig.s S9-S11).³ Thus, substitution of azido ligands in complex **1** (265°C) by tetrazolato ligands leads to a decrease in the decomposition onset temperatures.

³ The DSC traces can be found in the ESI.

The heats of decomposition, ΔH_{dec} , were found to be 1.4 kJ g^{-1} , 1.3 kJ g^{-1} and 1.5 kJ g^{-1} , respectively. They are markedly smaller than those of the tetraazido complexes **1** and **2** (2.4 and 2.3 kJ g^{-1}). A comparison of the molar heats of decomposition with the latter⁵² and the related compounds $\text{Ge}(\text{N}_3)_4(\text{L}_2)$, $\text{L} = \text{bpy}$, phen ,⁵⁸ and $(\text{PPN})_n\text{E}(\text{N}_3)_6$, $\text{E} = \text{P}$,⁵⁷ Si ,⁵¹ Ge ,⁵⁷ reveals that while each azido ligand contributes 176 – 224 kJ mol^{-1} to the molar heats of decomposition, the contribution from the tetrazolato ligands, is considerably lower (90 – 137 kJ mol^{-1}).

DFT calculations. On the example of the computationally less expensive mtz complexes, density functional theory calculations at the B3LYP/6-311G(d,p) level using the Gaussian03 package of programmes (see SI for full citation) were performed in order to assess the relative energies of geometrical and linkage isomers. Vibrational frequency calculations were used to establish the nature of optimised geometries and obtain temperature-dependent Gibbs energies was made into the internal energies of the complexes (see Table 4, Fig. 5). The molecular structures found in the crystals of **4a**, **4b** and **9** were used as start geometries for the optimisations. It was found that the sum of electronic and thermal free energies of **4a** is 3.1 kJ mol^{-1} less than that of the linkage isomer **4b** at 298 K (3.6 kJ mol^{-1} at 355 K). According to this figure, the **4a** : **4b** ratio is predicted to be 3.5 which is close to the spectroscopic observation ($\Delta G(\text{obs}) \approx 0.4 \text{ kJ mol}^{-1}$, ratio ≈ 1.2). This is consistent with **4a** being the sterically less strained, dominant component of the equilibrium in MeCN.

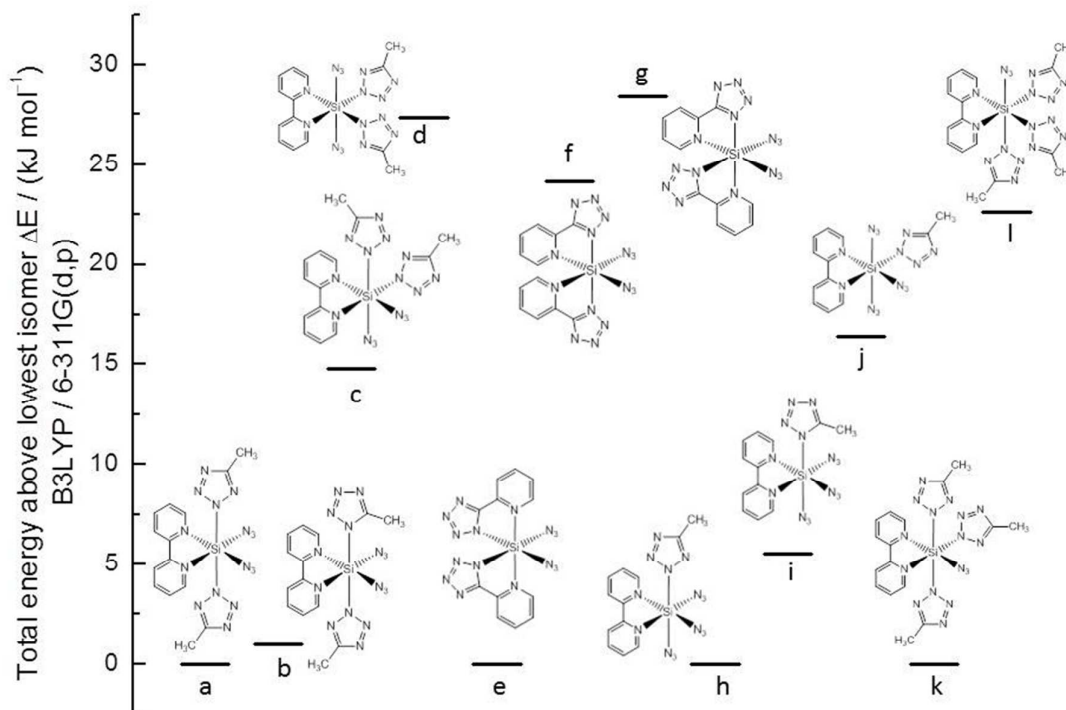


Fig. 5. Total energy differences as calculated by density functional theory at the B3LYP/6-311G(d,p) level of the complexes **4a** (a), **4b** (b), *OC-6-32-* (c) and *OC-6-33-[Si(N₃)₂(κN(2)-mtz)₂(bpy)]* (d), **9** *OC-6-22-* (e), *OC-6-13-* (f) and *OC-6-32-[Si(N₃)₂(κ²N,N(1)-pytz)₂]* (g), *OC-6-23-[Si(N₃)₃(κN(2)-mtz)(bpy)]* (h), *OC-6-23-[Si(N₃)₃(κN(1)-mtz)(bpy)]* (i) and *OC-6-33-[Si(N₃)₃(κN(2)-mtz)(bpy)]* (j), *OC-6-31-[Si(N₃)(κN(2)-mtz)₃(bpy)]* (k) and *OC-6-33-[Si(N₃)(κN(2)-mtz)₃(bpy)]* (l).

Table 4. Wavenumbers of the $\nu_{\text{as}}(\text{N}_3)$ vibrations of azido(5-methyltetrazolato) silicon complexes obtained from DFT calculations ^a

Complex	$\nu / (\text{cm}^{-1})$
<i>OC-6-12</i> -[Si(N ₃) ₄ (bpy)]	2285(1044), 2261(640), 2247(598), 2240(738) ^a
<i>OC-6-23</i> -[Si(N ₃) ₃ ($\kappa\text{N}(1)$ -mtz)(bpy)] (i)	2284(1238), 2256(362), 2240(512)
<i>OC-6-23</i> -[Si(N ₃) ₃ ($\kappa\text{N}(2)$ -mtz)(bpy)] (h)	2288(1006), 2268(757), 2252(547)
<i>OC-6-33</i> -[Si(N ₃) ₃ ($\kappa\text{N}(2)$ -mtz)(bpy)] (j)	2293(1092), 2263(933), 2257(110)
<i>OC-6-13</i> -[Si(N ₃) ₂ ($\kappa\text{N}(2)$ -mtz) ₂ (bpy)] (a)	2292(1055), 2272(518)
<i>OC-6-24</i> -[Si(N ₃) ₂ ($\kappa\text{N}(2)$ -mtz)($\kappa\text{N}(1)$ -mtz)(bpy)] (b)	2291(1125), 2255(212)
<i>OC-6-32</i> -[Si(N ₃) ₂ ($\kappa\text{N}(2)$ -mtz) ₂ (bpy)] (c)	2292(703), 2275(727)
<i>OC-6-33</i> -[Si(N ₃) ₂ ($\kappa\text{N}(2)$ -mtz) ₂ (bpy)] (d)	2287(1008), 2293(364)
<i>OC-6-22</i> -[Si(N ₃) ₂ ($\kappa^2\text{N},\text{N}(1)$ -pytz) ₂] (e)	2273(946), 2250(452)
<i>OC-6-32</i> -[Si(N ₃) ₂ ($\kappa^2\text{N},\text{N}(1)$ -pytz) ₂] (f)	2270(556), 2287(879)
<i>OC-6-31</i> -[Si(N ₃)($\kappa\text{N}(2)$ -mtz) ₃ (bpy)] (k)	2293(790)
<i>OC-6-33</i> -[Si(N ₃)($\kappa\text{N}(2)$ -mtz) ₃ (bpy)] (l)	2272(744)

^a bold letters in parentheses refer to Fig. 5; ^b oscillator strength / (km mol^{-1}) in parentheses.

An evaluation of the energies (Fig. 5) obtained from the calculations in the systems Si(N₃)₂(mtz)₂(bpy) and Si(N₃)₃(mtz)(bpy) reveals the $\kappa\text{N}(2)$ linkage isomers to be the energetically preferred coordination of the methyl tetrazolato ligands. Furthermore, the coordination of methyl tetrazolato ligands *trans* to the pyridine type ligand is energetically disfavoured. In the system Si(N₃)₂(pytz)₂, in which 5-(pyridin-2-yl)tetrazolato(1-) ligands (pytz) act as chelating ligands, the lowest energy stereoisomer has *OC-6-22* configuration with both tetrazolato- $\kappa\text{N}(1)$ ligands *trans* to an azido ligand. The combined evidence points toward steric control of the coordination configuration in which the bulkiest ligands prefer *trans* arrangement. These findings are in agreement with the experimentally observed slight excess of **4a** over **4b** in the equilibrium solution **4a,b**. Furthermore, the observed preference for *OC-6-22*-[Si(N₃)₂($\kappa^2\text{N},\text{N}(1)$ -pytz)₂] over the *OC-6-13* and *OC-6-33* isomers is corroborated experimentally. The calculations also indicate that *OC-6-23*-Si(N₃)₃($\kappa\text{N}(2)$ -mtz)(bpy) is the preferred intermediary complex in the reaction leading from **1** to **4a,b**. This intermediate (complex denoted as “**h**” in Fig. 5) has the lowest total energy in the series of candidates **h**, **i**, **j** and the predicted wavenumbers of the $\nu_{\text{as}}(\text{N}_3)$ vibrations of **h** (see Fig. S12 for calculated spectra of **1**, **h**, **i**, **j**) are in line with data obtained for the related complex **3** obtained in the reaction leading to **7** (Fig. 1). The experiments show that the isomers **4a,b** interconvert easily at 80°C. A transition state was found which links **4a** with **4b** (see Fig. 6). The vibration associated with the single imaginary frequency at -178 cm^{-1} describes the trajectory of a sigmatropic rearrangement of the tetrazolato ligand (Scheme 2). The energy barrier between the two linkage isomers was found to be 132 kJ mol^{-1} (at 298 K) above the groundstate of **4a**. The transition state connecting the $\kappa\text{N}(1)$ and $\kappa\text{N}(2)$ linkage isomers (TS1) is characterised by the coordination angle Si-N(1)-N(2) of 76° . A second transition state (TS2, Si-N(1)-N(2) = 170°) connects two conformers of complex **4a**. According to the reaction profile along

the Si-N(1)-N(2) angle, the energy barriers for both transformations are of approximately equal height.

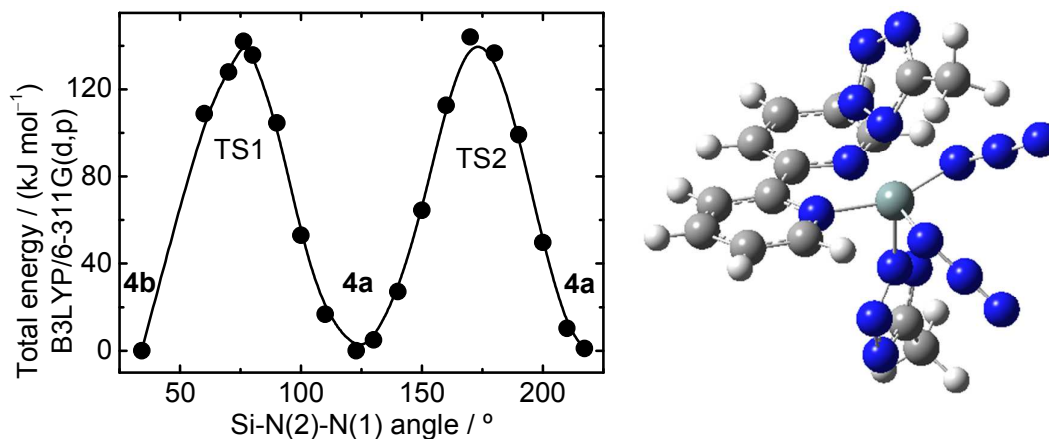


Fig. 6. Potential energy profile obtained by stepping the Si-N(2)-N(1) angle of a 5-methyl tetrazolato ligand in **4a**. The data point at *ca.* 75° marks the transition state connecting the linkage isomers **4a** and **4b** (left), ball-and-stick diagram of the transition state geometry connecting *OC-6-13*-[Si(N₃)₂(κN(2)-mtz)(bpy)] with *OC-6-24*-[Si(N₃)₂(κN(1)-mtz)(κN(2)-mtz)(bpy)], TS1, (right).

Scheme 2. Interconversion between the two linkage isomers *OC-6-13*-[Si(N₃)₂(κN(2)-mtz)₂(bpy)] (**4a**) and *OC-6-24*-[Si(N₃)₂(κN(1)-mtz)(κN(2)-mtz)(bpy)] (**4b**), and conformers of **4a**.

The dissociation of bpy, N₃⁻ or mtz⁻ or a pseudo rotation bringing about **4a/4b** interconversion all require more activation energy, hence the involvement of TS1 in the interconversion is highly likely.

Conclusion

The discussed work demonstrates a convenient route *via* sequential [3+2]-cycloaddition reactions to six-coordinate poly(tetrazolato) silicon species as a previously unknown complex type and the first isolated hyper-coordinate poly(tetrazolato) complexes of the element silicon with unequivocally determined structures. The new complexes have the potential for high nitrogen content with complex **9** having achieved 55% already. Thermally, the poly(tetrazolato) complexes are comparably robust (decomposing at temperatures above 200°C) but surprisingly less so than the related more energetic tetraazido complexes with which they share the same coordination skeleton. Even though the κN(2) linkage isomers are favoured thermodynamically due to steric crowding, the isomerism has been observed at elevated temperatures. The linkage isomerism was investigated further by DFT

calculations which revealed that *a*) the complex configuration is dominated by the ligand cone angles and that *b*) the reaction barriers of the two possible sigmatropic rearrangements of 5-methyltetrazolato ligands are of similar height. Introducing more than three tetrazolato ligands *via* cycloaddition reactions has thus far been futile and this is tentatively ascribed to the decreasing thermal stability upon increasing the number of covalently bound tetrazolato ligands. The synthesis of *homoleptic* tetrazolato silicon complexes will be the subject of a forthcoming paper.

Experimental Section

The starting complexes **1** and **2**·CH₃CN were synthesised using published procedures.⁵² Details of general experimental conditions and analytical equipment used can be found in the supplementary information of this paper. ¹H and ¹³C{¹H} NMR spectra were calibrated against the residual solvent proton resonance (1.94 ppm) or the natural abundance of ¹³C (118.3 ppm). Only the wavenumbers of the asymmetric N₃ stretching vibrations, $\nu_{\text{as}}(\text{N}_3)$, are quoted below; additional data available in the SI. Supplementary crystallographic data for this paper (CCDC 1493371, {(Ph₃P)₂N} Ph-CN₄; 1493372, **5**; 1493373, **6**·CH₃CN; 1493374, **7**·CH₃CN; 1493375, **4a**; 1493377, **9**; 1493376, **4b**·CH₃CN) can be obtained free of charge from the Cambridge Crystallographic Data Centre via www.ccdc.cam.ac.uk/data_request/cif.

In situ analytical data for [Si(N₃)₃(ptz)(bpy)] (3). A further 30 mg of a mixture of the complexes **5** and **3** was recovered by reduction in volume of washings and further cooling. The following analytical data of the two component mixture were assigned to complex **3**: IR $\bar{\nu}$ / (cm⁻¹) = 2152vs, 2117s (nujol). TOF MS ES⁺ (CH₃CN) *m/z* = 933 (100) [M₂ + Na], 634 (33) [M + Na(bpy)], 478 (94) [M + Na], 310 (41) [M – N₄CPh], 179 (24) [Na(bpy)]. ¹H NMR (250 MHz, r.t., CD₃CN, ppm) δ = 9.70 (2H, ddd, 5.9 Hz, 1.4 Hz, 0.8 Hz), 8.56 (2H, d), 8.49 (2H, m), 8.03 (2H, m), 7.81 (2H, m), 7.38 (3H, m).

Preparation of [Si(N₃)₂(mtz)₂(bpy)] (4a,b). An ampoule was charged with compound **1** (0.200 g, 0.568 mmol) and acetonitrile (ca. 10 ml). The reaction vessel was sealed and then fully immersed in oil bath set at a temperature of 90°C. The reaction mixture was stirred. In regular intervals, the reaction vessel was cooled to r.t. and *in situ* FTIR spectra were recorded. Initially a colourless clear solution, the reaction mixture converted in the course of four days into a white suspension, which was filtered hot (ca. 70°C) and the small filter residue was discarded. The volume of the filtrate was reduced to ca. 2 mL, which induced crystallisation. Crystallisation in the resultant suspension was completed by cooling overnight to –25°C. The supernatant solution was then filtered off and the filter residue washed with cold acetonitrile and dried *in vacuo*, which afforded a white solid (179 mg, 0.412 mmol, 73 %) of a mixture of OC-6-13-[Si(N₃)₂(κ N(2)-mtz)₂(bpy)] (**4a**) and OC-6-24-[Si(N₃)₂(κ N(1)-mtz)(κ N(2)-mtz)(bpy)] (**4b**), mp. 231-232°C, IR $\bar{\nu}$ / (cm⁻¹) = 2163vs, 2132w (CH₃CN). Separation of the linkage isomers can be accomplished by slow recrystallisation from MeCN. Note: heating of

MeCN solutions of either linkage isomer rapidly reforms the mixture of linkage isomers with a ratio of ca. 1 : 1. Elemental Analysis, 434.45 g mol⁻¹, C₁₄H₁₄N₁₆Si, calcd. C, 38.70; H, 3.25; N, 51.58%; found C, 38.71; H, 2.96; N, 51.40%.

Spectroscopic data for complex 4a. ¹H NMR (400 MHz, r.t., CD₃CN, ppm) δ = 9.84 (2H, d, 5.9 Hz), 8.48-8.46 (4H, m), 8.01-7.98 (2H, m), 2.20 (6H, s). ¹³C {¹H} NMR (100.6 MHz, r.t., CD₃CN, ppm) δ = 161.3 (mtz, κN(2)), 148.8, 146.2, 144.7, 129.2, 123.5, 10.7 (CH₃, κN(2)). IR $\bar{\nu}$ / (cm⁻¹) = 2149, 2122 (nujol).

Spectroscopic data for complex 4b. ¹H NMR (400 MHz, r.t., CD₃CN, ppm) δ = 9.59 (2H, d, 6.0 Hz), 8.56 (2H, d, 7.5 Hz), 8.52-8.47 (2H, m), 7.96-7.93 (2H, m), 2.80 (3H, s), 2.21 (3H, s). ¹³C {¹H} NMR (100.6 MHz, r.t., CD₃CN, ppm) δ = 167.3 (mtz, κN(1)), 161.3 (mtz, κN(2)), 148.1, 146.3, 145.5, 129.4, 123.5, 12.3 (CH₃, κN(1)), 10.7 (CH₃, κN(2)). IR $\bar{\nu}$ / (cm⁻¹) = 2157, 2122 (nujol).

Preparation of OC-6-13-[Si(N₃)₂(κN(2)-ptz)₂(bpy)] (5). A Schlenk tube was charged with Si(N₃)₄(bpy) (**1**, 106 mg, 0.301 mmol) and benzonitrile (ca. 25 ml), which formed a colourless and clear solution. The reaction vessel was immersed into a pre-heated oil bath and first heated at 150°C for 55 min and then heated at 140°C for another 25 min while the solution was stirred. During the heating periods IR spectra of the reaction solution were recorded in regular intervals which showed the gradual replacement of the $\nu_{\text{asym}}(\text{NN})$ bands of the starting material at 2148, 2120, 2113 cm⁻¹ by those of a product mixture at 2157, 2128, 2114 cm⁻¹. The solvent was then distilled off in vacuo and all remaining volatiles evaporated in high vacuum (1×10⁻³ mbar) affording a solid raw product (157 mg, 93% raw yield). Recrystallisation from hot acetonitrile afforded white, solid, analytically pure **5** (74 mg, 0.13 mmol 43% yield), m.p. 230-231°C (dec.). Elemental Analysis C₂₄H₁₈N₁₆Si, 558.61 g mol⁻¹, calcd. C, 51.60; H, 3.25; N, 40.12%; found C, 51.31; H, 3.17; N, 39.90%. ¹H NMR (250 MHz, r.t., CD₃CN, ppm) δ = 9.94 (H-6, 2H, ddd, 6.0 Hz, 1.3 Hz, 0.9 Hz), 8.51-8.49 (H-3 and H4, 4H, m), 8.03 (H-5, 2H, ddd, 6.1 Hz, 6.0 Hz, 2.9 Hz), 7.89-8.85 (H-2', 4H, m), 7.47-7.42 (H-3' and H-4', 6H, m). ¹³C {¹H} NMR (100 MHz, r.t., CD₃CN, ppm) δ = 163.8 (ptz), 149.0 (bpy), 146.3 (bpy), 145.0 (bpy), 130.6 (ptz), 129.8 (ptz), 129.6 (ptz), 129.3 (bpy), 127.4 (ptz), 123.7 (bpy). ²⁹Si NMR (99.34 MHz, r.t., ppm) δ = -190.4 ppm. TOF MS ES⁺ (CH₃OH) *m/z* = 1139 (3) [M₂ + Na], 971 (32) [M₂ - N₄CPh], 597 (2) [M + K], 581 (48) [M + Na], 548 (26) [M - N₃ + MeOH]. TOF MS ES⁺ (CH₃CN) *m/z* = 1139 (63) [M₂ + Na], 737 (7) [M + Na(bpy)], 597 (1) [M + K], 581 (47) [M + Na]. IR $\bar{\nu}$ / (cm⁻¹) = 2164vs, 2134w (CH₂Cl₂); 2162vs, 2132w (CH₃CN); 2163vs, 2129m (THF); 2166(63), 2126(32) (nujol).

Preparation of OC-6-13-[Si(N₃)₂(κN(2)-ttz)₂(bpy)]·CH₃CN (6). Compound **6** was synthesised and isolated (0.77 g, 66% of analytically pure material) using the conditions described for compound **5**. *M* = 627.71 g mol⁻¹, mp. 212°C (dec.). Elemental analysis of the MeCN free sample C₂₆H₂₂N₁₆Si,

calcd. C, 53.23; H, 3.78; N, 38.20%; found C, 53.29; H, 3.89; N, 38.68%. ^1H NMR (250 MHz, r.t., CD_3CN ppm) δ = 9.92 (H-6, 2H, d, 6.3 Hz), 8.48 (H-3 and H4, 4H, m), 8.01 (H-5, 2H, ddd, 5.9 Hz, 5.9 Hz, 3.1 Hz), 7.74 (H-2' and H-6', 4H, d, 8.2 Hz), 7.23 (H-3' and H-5', 4H, d, 8.2 Hz), 2.34 ($\text{CH}_3\text{-C}_4\text{H}_6$, 6H, s), 1.96 (CH_3CN , 3 H, s). ^1H NMR (250 MHz, r.t., CDCl_3 ppm) δ = 10.08 (H-6, 2H, ddd, 5.9 Hz, 1.5 Hz, 0.7 Hz), 8.34 (H-3, 4H, pseudo-t, 7.8 Hz, 1.5 Hz), 8.23 (H-2, 2H, ddd, 8.0 Hz, 1.2 Hz, 0.8 Hz), 7.93 (H-5, 2H, ddd, 7.6 Hz, 6.0 Hz, 1.3 Hz), 7.89 (H-2' and H-6', 4H, d, 8.1 Hz), 7.18 (H-3' and H-5', 4H, d, 7.9 Hz), 2.35 (CH_3 , 6H, s), 2.01 (CH_3CN , 3H, s). TOF MS ES^+ (CH_3CN) m/z = 1211 (42) [$\text{M}_2 + \text{K}$], 625 (100) [$\text{M} + \text{K}$], 195 (8) [bpy + K]. IR $\bar{\nu}$ / (cm^{-1}) = 2164vs, 2134w (CH_2Cl_2); 2162vs, 2133w (CH_3CN); 2162vs, 2132w (THF, cm^{-1}); 2156, 2127 (nujol).

Preparation of $OC\text{-}6\text{-}13\text{-}[\text{Si}(\text{N}_3)_2(\kappa\text{N}(2)\text{-ptz})_2(\text{phen})]\cdot\text{CH}_3\text{CN}$ ($7\cdot\text{CH}_3\text{CN}$). A Schlenk tube was charged with the hemisolvate $2\cdot 0.5\text{CH}_3\text{CN}$ (150 mg, 0.378 mmol) and heated at 110°C under dynamic vacuum until all acetonitrile had evaporated. The resulting acetonitrile-free compound was then dissolved in benzonitrile (ca. 20 mL) and heated under stirring for a total of 120 hours in an oil bath set at 120°C . At regular intervals, the reaction vessel was removed from the bath and a sample taken from the reaction mixture after it had cooled to r.t. for the purpose of IR spectroscopic monitoring the reaction. The yellow reaction solution was then diminished under a dynamic vacuum to afford an intractable oil, which was washed twice hexane (2 x 10 ml) resulting in a grey solid. The solid wash residue was dried in HV at 100°C and re-dissolved in a minimum volume of warm CH_3CN and filtered. Cooling the yellow filtrate at -28°C afforded pale yellow crystals of $7\cdot\text{CH}_3\text{CN}$, which were filtered off, washed (CH_3CN , 15 ml) and dried in vacuo in the cold, 83 mg (0.13 mmol, 35%). Analytically pure compound was obtained by re-crystallisation from CH_3CN . $M = 623.68 \text{ g mol}^{-1}$, mp. ca. 201°C (dec.). Elemental Analysis $\text{C}_{28}\text{H}_{21}\text{N}_{17}\text{Si}$, calcd. C, 53.92; H, 3.39; N, 38.18%; found C, 53.60; H, 3.29; N, 38.03%. ^1H NMR (500 MHz, r.t., CD_3CN , ppm) δ = 10.17 (H-2, 2H, dd, 5.5 Hz, 1.3 Hz), 9.00 (H-4, 2H, dd, 8.3 Hz, 1.3 Hz), 8.31 (H-3, 2H, dd, 8.3 Hz, 5.5 Hz), 8.23 (H-5, 2H, s), 7.74 (H-2', 4H, m), 7.34 (H-3', H4', 6H, m), 1.95 (CH_3CN , 3H, s). $^{13}\text{C}\{^1\text{H}\}$ NMR (62.8 MHz, r.t., CD_3CN , ppm) δ = 163.7, 149.7, 144.6, 136.0, 130.5, 129.7, 129.5, 128.3, 127.7, 127.3. IR $\bar{\nu}$ / (cm^{-1}) = 2162vs, 2132w (CH_3CN); 2164vs(sh), 2158vs, 2129s (nujol).

Preparation of $[\text{Si}(\text{N}_3)(\text{mtz})_3(\text{bpy})]$ (8**).** An ampoule was charged with compound **1** (162 mg, 0.460 mmol) and acetonitrile (ca. 10 mL). The reaction vessel was immersed into a pre-heated oil bath and heated at 90°C . Monitoring the reaction solution by in-situ FTIR spectroscopy of the reaction solution showed the gradual decrease of the intensity of the $\nu_{\text{as}}(\text{N}_3)$ absorption bands of **4a,b** at 2163 cm^{-1} (vs) and 2132 cm^{-1} (w). After a total of ten days an off white solid had precipitated and the originally clear and colourless solution had turned brown. The reaction mixture was filtered and the filtrate collected. The filtrate and washings contain a mixture of compound **8** and the intermediate linkage isomers **4a,b**. The filter residue was washed with acetonitrile (2 x 10 mL) at r.t. and with THF (10 mL) at 50°C

before being dried in *vacuo* to give compound **5** as a grey-cream coloured solid (118 mg, 0.247 mmol, 54%), mp. 225-227°C (dec.). Analysis calcd. C₁₆H₁₇N₁₇Si, 477.52 g mol⁻¹, C, 40.41; H, 3.60; N, 50.09%, found C, 39.98; H, 3.48; N, 49.39%. ¹H NMR (250 MHz, r.t., CD₃CN, ppm) δ = 9.84 (H6, dd, 1H), 8.63 (H6', 1H, dd), 8.60 (H5', 1H, ddd), 8.52 (H3, dd, 1H), 8.41 (H4, 1H, ddd), 8.22 (H3', 1H, d), 7.91 (H5, dd, 1H), 7.91 (H4', 1H, ddd); ³J(H3,H4) = 8.0 Hz, ³J(H3',H4') = 6.0 Hz, ⁴J(H3,H5) = 1.3 Hz, ⁴J(H3',H5') = 1.2 Hz, ³J(H4,H5) = 7.6 Hz, ³J(H4',H5') = 7.3 Hz, ⁴J(H4,H6) = 1.5 Hz, ⁴J(H4',H6') = 2.2 Hz, ³J(H5,H6) = 6.0 Hz, ³J(H5',H6') = 8.1 Hz; assignments are tentative; solubility insufficient for conclusive ¹³C{¹H} data. TOF MS ES⁺ (CH₃CN) *m/z* = 973 (29) [M₂ + Na], 498 (100) [M + Na], 157 (23) [bpy + H]. IR $\bar{\nu}$ / (cm⁻¹) = 2159vs (CH₃CN); 2158vs (THF); 2161vs (pyridine); 2158vs (nujol).

Preparation of OC-6-22-[Si(N₃)₂(κ²N(1),N'-pytz)₂] (9). A Schlenk tube was charged with compound **1** (200 mg, 0.568 mmol) and 2-cyanopyridine (1.703 g, 16.4 mmol). The reaction vessel was heated at 120°C for 12 hours before unreacted 2-cyanopyridine was distilled off in *vacuo* at 40°C. Residual 2-cyanopyridine and bpy was removed by washing with MeCN (3 mL) to yield compound **9** as an off-white solid (0.20 g, 0.49 mmol, 87%). Mp. 215-220°C (dec.). Elemental Analysis C₁₂H₈N₁₆Si, 404.39 g mol⁻¹, calcd. C, 35.64; H, 1.99; N, 55.42%; found C, 35.65; H, 1.81; N, 51.39%. ¹H NMR (250 MHz, r.t., CD₃CN, ppm) δ = 9.58 (2H, d, 5.6 Hz), 8.71 (2H, pdt, 7.8 Hz, 1.2 Hz), 8.58 (2H, d, 7.8 Hz), 8.19 (2H, ddd, 7.8 Hz, 5.8 Hz, 1.3 Hz). ¹H NMR (250 MHz, r.t., C₅D₅N, ppm) δ = 9.91 (2H, ddd, 5.8 Hz, 1.2 Hz, 0.8 Hz), 8.71 (2H, ddd, 0.9 Hz), 8.61 (2H, pdt, 7.8 Hz, 1.4 Hz), 8.14 (2H, ddd, 7.7 Hz, 5.8 Hz, 1.4 Hz). ¹³C{¹H} NMR (62.8 MHz, r.t., C₅D₅N, ppm) δ = 147.8, 146.7, 140.6, 128.4 (due to poor solubility the resonances of the two ipso C atoms were not observed). EI⁺ *m/z* = 362 (60) [M - N₃], 306 (15) [M - N₃ - 2N₂], 258 (12) [M - N₄C-C₅H₄N], 216 (13) [M - N₄C-C₅H₄N - N₃], 188 (35) [M - N₄C-C₅H₄N - N₃ - N₂], 156 (38) [bpy], 146 (75) [N₄C-C₅H₄N], 104 (75) [NC-py], 78 (100) [py]. IR $\bar{\nu}$ / (cm⁻¹) = 2143s(br) (CH₃CN); 2141s(br) (CH₂Cl₂), 2164(vs), 2122(s) (nujol).

Characteristic ¹H NMR data (250 MHz, r.t., CD₃CN, ppm) for the protons H6, H6' (bpy) and H2, H9 (phen) of the complexes studied *in situ* and of the starting complexes **1** and **2** for reference (H6,H6' and H2,H9 are isochronous, respectively): OC-6-22-[Si(N₃)₄(bpy)], δ = 9.40 (2H, ddd, 5.8, 1.5, 0.8 Hz); OC-6-23-[Si(N₃)₃(κN(1)-mtz)(bpy)], δ = 9.32 (2H, pd); OC-6-23-[Si(N₃)₃(κN(2)-mtz)(bpy)], δ = 9.64 (2H, pd); OC-6-32-[Si(N₃)₂(κN(2)-mtz)₂(bpy)], δ = 9.72 (1H); OC-6-23-[Si(N₃)₃(ttz)(bpy)], δ = 9.69 (2H, ddd) (CDCl₃, 9.84 (2H, ddd)); OC-6-22-[Si(N₃)₄(phen)], δ = 9.60 (2H, dd, 5.4, 1.3 Hz); OC-6-24-[Si(N₃)₂(κN(1)-mtz)(κN(2)-mtz)(phen)], δ = 9.85 (2H, d, 5.4 Hz); OC-6-13-[Si(N₃)₂(κN(2)-mtz)-₂(phen)], δ = 10.07 (2H, d, 5.5 Hz); OC-6-23-[Si(N₃)₃(κN(1)-mtz)(phen)], δ = 9.57 (2H, pd, ca. 5.5 Hz); OC-6-23-[Si(N₃)₃(κN(2)-mtz)(phen)], δ = 9.85 (2H); OC-6-23-[Si(N₃)₂(κN(2)-mtz)(phen)], δ = 9.93 (1H); OC-6-23-[Si(N₃)₃(ptz)(phen)], δ = 9.90 (2H, dd, 5.5 Hz, 1.2 Hz).

Supporting information available containing spectroscopic, thermochemical, crystallographic and computational data.

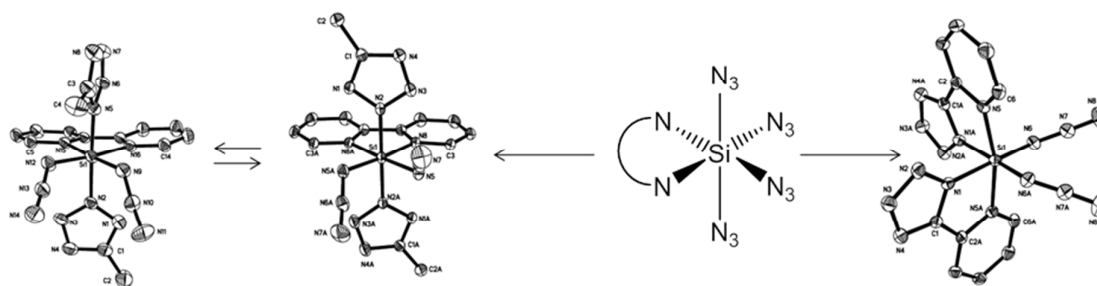
Acknowledgements. The authors acknowledge the support of the EPSRC for an advanced research fellowship (PP, E054978/1) and postdoctoral fellowship (MD) and the University of Sheffield. H. Adams, B. Peerless and S. von Meurs are thanked for their assistance with the crystallographic and NMR investigations.

References

- 1 I. Kobrsi, W. Zheng, J. E. Knox, M. J. Heeg, H. B. Schlegel, C. H. Winter *Inorg. Chem.* 2006, **45**, 8700-8710.
- 2 E. S. Andreiadis, R. Demadrille, D. Imbert, J. Pecaut, M. Mazzanti *Chem. Eur. J.* 2009, **15**, 9458-9476.
- 3 E. A. Popova, R. E. Trifonov, V. A. Ostrovskii *ARKIVOC* 2012, 45-65.
- 4 M. Seredyuk, L. Piñeiro-López, M. C. Muñoz, F. J. Martínez-Casado, G. Molnár, J. A. Rodríguez-Velamazán, A. Bousseksou, J. A. Real *Inorg. Chem.* 2015, **54**, 7424-7432.
- 5 T. V. Serebryanskaya, T. Yung, A. A. Bogdanov, A. Shchebet, S. A. Johnsen, A. S. Lyakhov, L. S. Ivashkevich, Z. A. Ibrahimava, T. S. Garbuzenco, T. S. Kolesnikova, N. I. Melnova, P. N. Gaponik, O. A. Ivashkevich *J. Inorg. Biochem.* 2013, **120**, 44-53.
- 6 Z. Du, Y. Zhang, Z. Han, Q. Yao *Propell. Explos. Pyrotech.* 2015, **40**, 954-959.
- 7 M. H. V. Huynh, M. D. Coburn, T. J. Meyer, M. Wetzler *Proc. Natl. Acad. Sci. USA* 2006, **103**, 10322-10327.
- 8 D. Lu, C. H. Winter *Inorg. Chem.* 2010, **49**, 5795-5797.
- 9 G. Steinhauser, T. M. Klapötke *Angew. Chem., Int. Ed.* 2008, **47**, 2-20.
- 10 R. Singh, R. D. Verma, D. T. Meshri, J. M. Shreeve *Angew. Chem., Int. Ed.* 2008, **47**, 3330-3347.
- 11 K. Karaghiosoff, T. M. Klapötke, C. M. Sabate *Eur. J. Inorg. Chem.* 2009, **238-250**.
- 12 T. M. Klapötke, C. M. Sabate, J. M. Welch *Eur. J. Inorg. Chem.* 2009, 769-776.
- 13 T. M. Klapötke, C. M. Sabate *New J. Chem.* 2009, **33**, 1605-1617.
- 14 M. H. V. Huynh, M. A. Hiskey, T. J. Meyer, M. Wetzler *Proc. Natl. Acad. Sci. U.S.A.* 2006, **103**, 5409-5412.
- 15 C. Ye, J.-C. Xiao, B. Twamley, J. M. Shreeve *Chem. Commun.* 2005, 2750-2752.
- 16 H. Xue, Y. Gao, B. Twamley, J. M. Shreeve *Inorg. Chem.* 2005, **44**, 5068-5072.
- 17 G. Steinhauser, T. M. Klapötke *Angew. Chem. Int. Ed.* 2008, **47**, 3330.
- 18 H.-L. Zhu, F.-D. Han, J.-Q. Bi, Y.-J. Bai, Y.-X. Qi, L.-L. Pang, C.-G. Wang, S.-J. Li *J. Am. Ceram. Soc.* 2009, **92**, 535-538.
- 19 M. V. Werrett, D. Chartrand, J. D. Gale, G. S. Hanan, J. G. MacLellan, M. Massi, S. Muzzioli, P. Raiteri, B. W. Skelton, M. Silberstein, S. Stagni *Inorg. Chem.* 2011, **50**, 1229-1241.
- 20 A. Palazzi, S. Stagni, S. Selva, M. Monari *J. Organomet. Chem.* 2003, **669**, 135-140.
- 21 I. Gronde, N. W. Mitzel *Z. Anorg. Allg. Chem.* 2009, **635**, 1313-1320.
- 22 J. Wagler, U. Böhme, E. Brendler, B. Thomas, S. Goutal, H. Mayr, B. Kempf, G. Y. Remennikov, G. Roewer *Inorg. Chim. Acta* 2005, **358**, 4270-4286.
- 23 C. Janiak, T. G. Scharmann, K. W. Brzezinka, R. Reich *Chem. Ber.* 1995, **128** 323-328.
- 24 W. P. Fehlhammer; W. Beck *Z. Anorg. Allg. Chem.* 2013, **639**, 1053-1082; W. P. Fehlhammer, W. Beck *Z. Anorg. Allg. Chem.* 2015, **641**, 1599-1678; P. Portius; M. Davis *Coord. Chem. Rev.* 2013, **257**, 1011-1025; V. Y. Kukushkin, A. J. L. Pombeiro *Chem. Rev.* 2002, **102**, 1771-1802 and lit. cited therein.
- 25 H.-W. Frühauf *Chem. Rev.* 1997, **97**, 523-596.
- 26 V. Aureggi, G. Sedelmeier *Angew. Chem. Int. Ed.* 2007, **46**, 8440-8444.
- 27 M. Begtrup, P. Larsen *Acta Chim. Scand.* 1990, **44**, 1050-1057.

- 28 A. Alvanipour, N. H. Buttrus, C. Eaborn, P. B. Hitchcock, A. I. Mansour, A. K. Saxena *J. Organomet. Chem.* 1988, **349**, 29-36.
- 29 C. Wentrup, S. Fischer, A. Maquestiau, R. Flammang *Angew. Chem.* 1985, **97**, 74-75.
- 30 E. Ettenhuber, K. Ruehlmann *Chem. Ber.* 1968, **101**, 743-750.
- 31 L. Birkofer, A. Ritter, P. Richter *Chem. Ber.* 1963, **96**, 2750-2757.
- 32 L. A. Lazukina, V. P. Kukhar *Zh. Org. Khim.* 1979, **15**, 2216-2217.
- 33 A. D. Sinitsa, N. A. Parkhomenko, L. N. Markovskii *Zh. Obshch. Khim.* 1977, **47**, 232.
- 34 N. Wiberg, G. Schwenk *Chem. Ber.* 1971, **104**, 3986-3988.
- 35 D. R. Haines, N. J. Leonard, D. F. Wiemer *J. Org. Chem.* 1982, **47**, 474-482.
- 36 P. Pelouquin, D.M.; Schmedake, T.A. Recent advances in hexacoordinate silicon with pyridine-containing *Coord. Chem. Rev.* 2016, **323**, 107-119.
- 37 A. A. Korlyukov *Russ. Chem. Rev.* 2015, **84**, 422-440.
- 38 J. Wagler, U. Böhme, E. Kroke *Structure and Bonding* D. Scheschkewitz (ed). Springer: Berlin, Germany, 2014, **155**, 29-105.
- 39 W. Levason, G. Reid, W. Zhang *Coord. Chem. Rev.* 2011, **255**, 1319-1341.
- 40 K. Junold, C. Burschka, R. Bertermann, R. Tacke *Dalton Trans.* 2010, **39**, 9401-9413.
- 41 C. Chuit; R. J. P. Corriu; C. Reye *Chemistry of Hypervalent Compounds* K.-y. Akiba (ed.), Wiley, 1999, 81-146.
- 42 N. Jagerovic, J.-M. Barbe, M. Farnier, R. Guillard *J. Chem. Soc. Dalton Trans.* 1988, 2569-2571.
- 43 W. Holzer, C. Jaeger *Monatsh. Chem.* 1992, **123**, 1027-1036.
- 44 M. Begtrup, J. Elguero, R. Faure, P. Camps, C. Estopa, D. Ilavsky, A. Fruchier, C. Marzin, J. De Mendoza *Magn. Reson. Chem.* 1988, **26**, 134-151.
- 45 A. Könnecke, E. Kleinpeter *Org. Magn. Resonance* 1979, **12**, 667-672.
- 46 D. A. Wann, I. Gronde, T. Foerster, S. A. Hayes, S. L. Masters, H. E. Robertson, N. W. Mitzel, D. W. H. Rankin *Dalton Trans.* 2008, **3817-3823**.
- 47 J. Wessel, U. Behrens, E. Lork, R. Mews *Angew. Chem. Int. Ed.* 1995, **34**, 443-446.
- 48 A. V. Kalinin, E. T. Apasov, S. L. Ioffe, V. P. Kozyukov, V. P. Kozyukov *Izv. Akad. Nauk SSSR Ser. Khim.* 1985, 1447-1449.
- 49 H. Bock, R. Dammel, S. Fischer, C. Wentrup *Tetrahedron Lett.* 1987, **28**, 617-620.
- 50 E. Wiberg, H. Michaud *Z. Naturforsch. B* 1954, **9**, 500.
- 51 A. C. Filippou, P. Portius, G. Schnakenburg *J. Am. Chem. Soc.* 2002, **124**, 12396-12397.
- 52 P. Portius, A. C. Filippou, G. Schnakenburg, M. Davis, K.-D. Wehrstedt *Angew. Chem. Int. Ed.* 2010, **49**, 8013-8016.
- 53 E. G. Rochow *Pure Appl. Chem.* 1966, **13**, 247-262.
- 54 U. Wannagat *Adv. Inorg. Chem. Rad.* 1964 (Ed. Emeleus), **6**, 225-274.
- 55 R. Fessenden, J. S. Fessenden *Chem. Rev.* 1961, **61**, 361-388.
- 56 P. Neugebauer, B. Jaschke, U. Klingebiel *The Chemistry of Organic Silicon Compounds, Patai's Chemistry of Functional Groups* (eds Z. Rappoport and Y. Apeloig), John Wiley & Sons Ltd., 2009, **3**.
- 57 P. Portius, P. W. Fowler, H. Adams, T. Z. Todorova *Inorg. Chim. Acta* 2008, **47**, 12004-12009.
- 58 A. C. Filippou, P. Portius, D. U. Neumann, K.-D. Wehrstedt *Angew. Chem. Int. Ed.* 2000, **39**, 4333-4336.
- 59 E. Bär, W. P. Fehlhammer, D. K. Breitinger, J. Mink *Inorg. Chim. Acta* 1984, **82**, L17.
- 60 W. Heininger, R. Stucka, G. Nagorsen *Z. Naturforsch. B* 1986, **41**, 702-707.
- 61 W. Heininger, K. Polborn, G. Nagorsen *Z. Naturforsch. B* 1988, **43**, 857-861.
- 62 M. Fritz, D. Rieger, E. Bär, G. Beck, J. Fuchs, G. Holzmann, W. P. Fehlhammer *Inorg. Chim. Acta* 1992, **198-200**, 513.
- 63 R. Guillard, N. Jagerovic, J. M. Barbe, Y. H. Liu, L. Perrot, C. Naillon, E. V. Caemelbecke, K. M. Kadish *Polyhedron* 1995, **14**, 3041.
- 64 A. C. Filippou, P. Portius, G. Kociok-Köhn *J. Chem. Soc. Chem. Comm.* 1998, 2327-2328.
- 65 W. R. Ellis, W. L. Purcell *Inorg. Chem.* 1982, **21**, 834-837.
- 66 D. Cantillo, B. Gutmann, C. O. Kappe *J. Am. Chem. Soc.* 2011, **133**, 4465-4475.

Table of contents Graphic**Synopsis**



The unusual situation presented by a silicon centre coordinating four 1,3-dipolar ligands is exploited in thermally activated cycloaddition reactions with nitriles that lead to six-coordinate poly(tetrazolato) complexes of silicon.